HHS Public Access

Author manuscript

Mol Cancer Res. Author manuscript; available in PMC 2017 May 01.

Published in final edited form as:

Mol Cancer Res. 2016 May ; 14(5): 482–492. doi:10.1158/1541-7786.MCR-15-0427.

STAT1 and NFκB Inhibitors Diminish Basal Interferon Stimulated Gene Expression and Improve the Productive Infection of Oncolytic HSV in MPNST cells

Joshua D. Jackson[1], **James M. Markert**[1,2,3], **Li Li**[1], **Steven L. Carroll**[4], and **Kevin A. Cassady**[2,5]

[1]Department of Neurosurgery, University of Alabama at Birmingham, Birmingham, AL 35233, USA

[2]Department of Pediatric, University of Alabama at Birmingham, Birmingham, AL 35233, USA

[3]Department of Cell, Developmental and Integrative Biology, University of Alabama at Birmingham, Birmingham, AL 35233, USA

[4]Department of Pathology and Laboratory Medicine, Medical University of South Carolina, Charleston, SC, 29425,USA

[5]Nationwide Children's Hospital and The Ohio State University, OH 43205, USA

Abstract

Interferon stimulated genes (ISGs) encode diverse proteins that mediate intrinsic antiviral resistance in infected cells. Here it was hypothesized that malignant peripheral nerve sheath tumor (MPNST) cells resist the productive infection of oncolytic herpes simplex virus (oHSV) through activation of the JAK/STAT1 pathway and resultant upregulation of ISGs. Multiple human and mouse MPNST cells were used to explore the relationship between STAT1 activation and the productive infection of Δγ-134.5 oHSVs. STAT1 activation in response to oHSV infection was found to associate with diminished Δγ-134.5 oHSVs replication and spread. Multi-day pre-treatment, but not co-treatment, with a JAK inhibitor significantly improved viral titer and spread. ISG expression was found to be elevated prior to infection and downregulated when treated with the inhibitor, suggesting that the JAK/STAT1 pathway is active prior to infection. Conversely, upregulation of ISG expression in normally permissive cells significantly decreased oHSV productivity. Finally, a possible link between NFκB pathway activation and ISG expression was established through the expression of inhibitor of kB (IκB) which decreased basal STAT1 transcription and ISG expression. These results demonstrate that basal ISG expression prior to infection contributes to the resistance of Δγ-134.5 oHSVs in MPNST cells.

CORRESPONDING AUTHOR: Kevin A. Cassady, M.D., Center for Childhood Cancer and Blood Diseases, The Research Institute at Nationwide Children's Hospital, The Ohio State University College of Medicine, 700 Children's Drive, Columbus, Ohio 43205, 614-722-2798, Kevin.Cassady@Nationwidechildrens.org.

CONFLICT OF INTEREST: JMM is a co-founder, stockholder and consultant for Catherex, Inc., which holds intellectual property related to oncolytic HSV.

Implications—While cancer-associated ISG expression has been previously reported to impart resistance to chemotherapy and radiotherapy, these data show that basal ISG expression also contributes to oncolytic HSV resistance.

Keywords

STAT1; ISG; NFκB; oHSV

Introduction

Malignant peripheral nerve sheath tumors (MPNSTs) are a highly aggressive cancer of the peripheral nervous system derived from cells of the Schwann cell lineage. Patients have a median survival of 26 months following diagnosis (1). Beyond advances in surgical resection, further treatment with chemotherapy and radiation has not demonstrated an overall benefit to survival (2, 3). A promising alternative approach is the use of conditional replicating oncolytic herpes simplex viruses type-1 (oHSVs) to treat MPNSTs. These oHSVs have been safely used in clinical trials in a number of cancer types, however, the tumor response has varied and we anticipate this would be true for patients with MPNSTs. We have previously demonstrated that MPNST cell lines exhibit variable oHSV susceptibility (4), and we have sought to understand the potential mechanisms of resistance that are detrimental to oHSV therapy.

Tumor resistance to oHSV has been attributed to oncogenic signaling cascade changes, namely Ras-mediated suppression of protein kinase R (PKR) in the infected cells (5). PKR is a host antiviral kinase that limits $\gamma_1$34.5 deleted oHSV late-gene expression and replication (6). In brief, HSV produces double-stranded RNA (dsRNA) during viral gene expression which induces PKR dimerization, auto-phosphorylation, and activation. Activated PKR phosphorylates eukaryotic initiation factor eIF2 alpha (eIF2α), leading to translational arrest in the infected cell. Wild-type HSV counters translational arrest by expressing the neurovirulence gene $\gamma_1$34.5 which encodes a multifunctional viral protein, infected cell protein 34.5 (ICP34.5). ICP34.5 recruits a host phosphatase, protein phosphatase 1 alpha (PP1α), to dephosphorylate eIF2α thus restoring protein translation in the infected cell. Though wild-type HSV causes lethal encephalitis in the central nervous system, deletion of one or both copies of the diploid $\gamma_1$34.5 gene attenuates neurogenic virulence. It is believed that malignant cells partially complement the loss of $\gamma_1$34.5 through oncogenic processes such as Ras-induced suppression of PKR.

In addition to PKR, cells express a diverse set of pattern recognition receptors (PRRs) that detect pathogen associated molecular patterns (PAMPs) such as viral nucleic acids. Stimulation of certain PRRs including DEAD (Asp-Glu-Ala-Asp) box polypeptide 58 (DDX58) (commonly known as retinoic acid-inducible gene I; RIG-I), interferon induced with helicase C domain 1 (IFIH1) (commonly known as melanoma differentiation antigen 5; MDA5), transmembrane protein 173 (TMEM173) (commonly known as stimulator of interferon genes; STING), and members of the toll-like receptor (TLR) family ultimately lead to the activation of transcription factors which promote expression of the Type-I interferons IFNα and IFNβ which are potent antiviral cytokines. Secreted Type-I IFN

interacts with transmembrane IFN-alpha receptors (IFNARs) in an autocrine and paracrine manner leading to the activation of the intracellular Janus kinases JAK1 and TYK2. Activation of JAK1 and TYK2 leads to phosphorylation of signal transducer and activator of transcription 1 (STAT1) and STAT2, which together with interferon regulatory factor 9 (IRF9) form the heterotrimeric transcription factor interferon stimulated gene factor 3 (ISGF3). The ISGF3 complex localizes to the nucleus where it promotes transcription of several hundred interferon stimulated genes (ISGs) that contain interferon stimulated response elements (ISREs) in their promoter regions. ISGs have diverse functions, modulating viral and cellular functions to promote intrinsic antiviral resistance. ISGs can directly inhibit mechanisms unique to certain viruses (e.g. myxovirus resistance 1, MX1), inhibit cellular processes involving transcription and translation (e.g. PKR; and 2'-5'-oligoadenylate synthetase 1, OAS1), or increased expression of PRRs and IFN/STAT1 signaling modulators to promote amplification of the antiviral response (e.g. RIG-I; MDA5; interferon-induced protein with tetratricopeptide repeats 3, IFIT3).

The research presented here tests the hypothesis that ISG upregulation contributes to oHSV resistance in a subset of MPNST tumor lines. Our results show that: (i) PKR activation is not specifically associated with oHSV resistant phenotypes; (ii) STAT1 activation is observed in 10 of 21 MPNST cell lines and is statistically associated with diminished productivity of both a first generation $\Delta\gamma_1$34.5 oHSV and a second generation $\Delta\gamma_1$34.5 oHSV, C134, capable of evading PKR-mediated translational arrest; (iii) resistant MPNST cell lines exhibit greater ISG expression than oHSV sensitive lines prior to oHSV infection suggesting they are primed toward an antiviral state; (iv) pre-treatment of resistant MPNST tumor lines with a small-molecule JAK inhibitor reduces basal ISG expression and improves viral replication and spread; (v) conversely, either IFN stimulation or stable ISGF3 overexpression in MPNST cell lines increased ISG expression leading to decreased oHSV productivity; and finally (vi) we have provided evidence that basal expression of ISGs may be dependent on the nuclear factor kappa-light-chain-enhancer of activated B cells (NFκB) signaling network.

Materials and Methods

Cell lines and viruses

Human MPNST cell lines or their firefly luciferase expressing derivatives (“-luc”) (4) as well as MPNSTs lines derived from a genetically engineered mouse model (7) have been previously described. All MPNST cell lines were maintained in growth media containing DMEM with 10% fetal bovine serum and 10 mM L-glutamine (Sigma). The African green monkey kidney cell line Vero was obtained from the ATCC and maintained in MEM with 5% bovine growth serum. All viruses except M201 have been previously described (4, 8) and are summarized in Supplemental Table 1. M201 is an oHSV with CMVp-GFP inserted between UL3 and UL4, and murine IL-12 inserted in $\gamma_1$34.5 locus and was constructed using homologous recombination with M002 (mIL-12 virus) viral DNA (8) and pCK1029 plasmid DNA using a method previously described (6). Sequential plaque purification was performed using Vero cells using EGFP expression and candidate viruses were verified by southern blot (data not shown).

Reagents

The small molecule inhibitors ruxolitinib and TPCA-1 (Selleckchem) were stored as 10mM aliquots in DMSO (Sigma). Primary antibodies were obtained as follows: p-T446-PKR (3076), p-S51-eIF2α (3398), eIF2α (2103), p-Y701-STAT1 (9167), STAT1 (9172), MDA5 (5321), RIG-I (3743), p-S536-NFκB/P65 (3033), NFκB/P65 (3987) IκB (4814), p-MEK1/2 (2338), MEK1/2 (4694), p-ERK1/2 (4376), and ERK1/2 (9102) from Cell Signaling; MX1 (13750), OAS1 (14955), IFIT3 (15201), STAT2 (16674), and IRF9 (14167) from Proteintech; HSV ICP4 (H1A021; Virusys), PKR (sc707; Santa Cruz) and β-actin (A2228; Sigma). Horseradish peroxidase (HRP) conjugated goat anti-mouse (Immunopore) and goat anti-rabbit antibodies were used as secondary antibodies.

Viral productivity assays

Viral recovery (replication) assays have been previously described (4) with the following modifications: Virus inoculation was performed in 150 μl regular growth media (10% FBS) for 1 hr followed by addition of growth media up to 1 mL per well in 24 well plates. Viral spread assays have been previously described (4). In brief, cells were seeded 1.5×10^5 per well in 24 well plates and infected at an MOI of 0.1 with GFP expressing viruses or mock infected (media alone). After 48 hrs, we performed flow cytometry to assess the percentage of cells positive for viral GFP. Flow Cytometry Absolute Count Standard fluorescent beads (Bangs Laboratories) were added to the final suspension of cells to calculate the ratio of cells surviving infection compared to mock infected samples. All samples were collected in triplicate and the means reported.

Lentivirus construction and transduction

Cloning methods and construction of lentivector plasmids are provided as supplemental information. Lentivirus production has been previously described (4). Stable cell lines were produced via lentiviral transduction of the target cell lines. Hygromycin (Sigma) selection (300 μg/ml) was applied no earlier than 48 hrs after transduction.

Western blotting

Cellular lysates were collected on ice in RIPA buffer (10 mM Tris-Cl pH 8.0, 1 mM EDTA, 1% Triton X100, 0.1% sodium deoxycholate, 0.1% SDS, 140 mM NaCl) with protease inhibitor cocktail (Roche) and diluted in 4x sample buffer (240 mM Tris-Cl pH 6.8, 40% glycerol, 4% SDS, 20% β-mercaptoethanol, 0.04% bromophenol blue). Samples were denatured at 98°C for five minutes, chilled on ice, separated by PAGE, and transferred to a nitrocellulose membrane (Thermo Scientific) and blocked for 1 hour at room temperature with 5% dry milk (S.T. Jerrell Co.) or bovine serum albumin (Fisher). Membranes were incubated overnight at 4°C with primary antibody diluted in Tris-buffered saline with 0.1% Tween-20 (TBST). Membranes were repeatedly washed with TBST, incubated for 1 hr with secondary antibody diluted in TBST (1:20,000) at room temperature, and subsequently washed with TBST. Membranes were wetted with SuperSignal West Pico Chemiluminescent Substrate (Thermo Scientific) and exposed to x-ray film (Research Products International).

Luciferase assays

The STS26T-luc and ST8814-luc cell lines used in reporter assays have been previously transduced with firefly luciferase under a constitutive CMV promoter. These cell lines were transduced via lentivirus with a nanoluciferase reporter (with a C-terminal PEST sequence) (Promega) under the control of either ISRE or NFκB promoters. Luminescence assays were performed in opaque 96-well plates with the Nano-Glo Dual Luciferase Reporter Assay (Promega) according to the manufacturer's instructions. Luminescence was measured using a FLUOStar Optima (BMG Labtech) plate reader. Nanoluciferase activity was normalized to that of firefly luciferase and reported as arbitrary units. Data were collected in triplicate or quadruplicate.

Statistical analysis

Statistical analysis was performed using Prism 5 (GraphPad Software). One-tailed Mann-Whitney U test was used for analysis involving multiple cell lines. Student's t test was used for inhibitor and transduction experiments within individual cell lines. For all analyses, the cutoff for statistical significance was set at $P<0.05$. The following notation was used: (ns) $P > 0.05$, (*) $P \leq 0.05$, (**) $P \leq 0.01$, (***) $P \leq 0.001$.

Results

PKR activation in response to oHSV infection

To assess the contribution of antiviral signaling pathways to oHSV resistance in MPNSTs, we assessed PKR activation and eIF2α phosphorylation in response to a $\Delta\gamma_1 34.5$ oHSV (R3616, kindly provided by Dr. Bernard Roizman, University of Chicago, Chicago, IL). The relevant characteristics of R3616 and other viruses used in the following experiments are provided in Supplemental Table 1. We first determined the susceptibility of 8 human and 13 mouse MPNST cell lines by viral recovery assay 24 hr after cells were infected at a multiplicity of infection (MOI) of 1. Titers of recovered virus ranged from 7.9×10^3 to 4.1×10^5 plaque forming units (PFU) for human cell lines and 1.5×10^3 to 2.0×10^5 PFU for mouse lines (Fig. 1 A–B). While mouse lines yielded 3-fold lower average titers of virus than human-derived lines (3.2×10^4 and 9.5×10^5 PFU respectively), the distributions of human and mouse lines were statistically indistinguishable (Supplemental Figure 1). Immunoblots against phosphorylated PKR (p-PKR) and p-eIF2α in human cell lines, or p-eIF2α in mouse cell lines, revealed PKR activation and eIF2α phosphorylation following R3616 infection (Fig 1 C–D) at 12 hpi in nearly all cell lines tested. There was no apparent difference in p-PKR/p-eIF2α between cell lines with high or low viral recovery. We conclude that activation of PKR is not sufficient to exclusively define the resistant phenotypes observed in MPNST cell lines.

Activation of STAT1 in response to oHSV infection and association with viral productivity

Because deletion of the HSV $\gamma_1 34.5$ gene increases HSV-1 sensitivity to Type-I IFNs (9) which activate STAT1, we hypothesized that oHSV-induced STAT1 activation was associated with decreased viral productivity in MPNST cells. We determined that 6 hpi was the optimal time to observe STAT1 Y701 phosphorylation (Supplementary Fig. 2). R3616

infection induced STAT1 activation in 3 of 8 (38%) human (Fig. 2A) and in 7 of 13 (54%) mouse cell lines (Fig. 2B). When exposed to exogenous IFNβ (200 IU/ml) STAT1 Y701 phosphorylation was evident in all human MPNST cell lines indicating that mechanisms for signal transduction were functional (Supplemental Fig. 3). When R3616 titers from all MPNST cell lines were sorted into STAT1 unresponsive (pSTAT1-) and STAT1 responsive (pSTAT1+) groups, cell lines which were STAT1 responsive were associated with significantly lower viral recovery (Fig. 2C). To further test the association of the STAT1 response of each cell line with viral productivity, we assessed viral spread within an *in vitro* monolayer. In this assay, the percentage of cells infected with an eGFP expressing $\Delta\gamma_1$34.5 virus (C101) in a multi-step infection (MOI=0.1, 48 hpi) was measured by flow cytometry. In general, MPNST cell lines tended to be resistant to the spread of C101 in the multi-step assay, however permissive cell lines which supported spread were associated with an unresponsive STAT1 phenotype (Fig. 2D). To determine if differences in STAT1 activation was cyto-protective following oHSV infection, we measured the number of gated cells by flow cytometry at 48 hpi following multi-step infection with C101 and compared the counts to mock infected cells. The results showed a trend toward higher cell counts (lower cytotoxicity) after C101 infection in STAT1 responsive cell lines, however, similar to the previous assessment, the majority of cell lines were resistant to the cytotoxic effects of C101 (Fig. 2E).

To identify if the STAT1 response was associated with diminished oHSV productivity in the setting of a $\Delta\gamma_1$34.5 oHSV capable of PKR evasion, we repeated the spread and cytotoxicity studies using C134, a chimeric $\Delta\gamma_1$34.5 oHSV expressing the human cytomegalovirus (HCMV) IRS1 gene product which inhibits PKR-mediated translational arrest. Immunoblots against PKR and eIF2α verified that C134 inhibited PKR-induced eIF2α phosphorylation in MPNST tumor cells (Fig 3A) similar to what has been observed in other cell lines (10). In a viral spread assay with C154 (an eGFP expressing variant of C134), we found that similar to the results with C101, the spread and cytotoxic effect of C154 was significantly diminished in STAT1 responsive cell lines (Fig3B and 3C). Next, to identify if the productivity of wild-type HSV-1 was associated with STAT1 response, we repeated the spread and cytotoxicity assays with a wild-type HSV-1(F) that expresses eGFP (M2001). The results show that unlike $\Delta\gamma_1$34.5 oHSVs, the STAT1 response was not significantly associated with wild-type HSV-1 spread or cytotoxicity in the MPNST cell lines (Fig. 3 D-E). Both viral spread and cytotoxicity induced by M2001 was generally high in all cell lines compared to the $\Delta\gamma_1$34.5 attenuated viruses.

These results demonstrate that the restricted productivity of $\Delta\gamma_1$34.5 oHSVs is significantly associated with the capacity of a cell to activate the STAT1 signaling cascade in response to $\Delta\gamma_1$34.5 oHSV infection. This association exists irrespective of PKR mediated translational arrest inasmuch as the spread and cytotoxicity of C134, a $\Delta\gamma_1$34.5 HSV capable of PKR evasion, is also restricted in these STAT1 responsive cell lines. In contrast, the productivity of wild-type HSV-1 was not associated with the capacity for a STAT1 response in similar assays.

Modulation of STAT1 activation by the JAK inhibitor ruxolitinib

Next, to determine whether the observed STAT1 activation was directly responsible for diminished $\Delta\gamma_1$34.5 viral productivity in resistant MPNST cell lines, we inhibited STAT1 Y701 phosphorylation using the JAK1/2 inhibitor ruxolitinib. We hypothesized that by inhibiting this response, $\Delta\gamma_1$34.5 oHSV productivity could be improved. To test this hypothesis, we treated the oHSV resistant MPNST cell lines STS26T-luc and ST8814-luc with 250 nM ruxolitinib (Rux) or vehicle (DMSO) following $\Delta\gamma_1$34.5 oHSV infection. Co-treatment with ruxolitinib did not improve $\Delta\gamma_1$34.5 oHSV infection and spread compared to DMSO in multi-step (low MOI) assay with C101 (Fig. 4A) despite the fact that ruxolitinib co-treatment prevented STAT1 Y701 phosphorylation (Fig. 4G). In viral recovery assays, ruxolitinib co-treatment did not improve R3616 replication in a single-step (MOI=1) assays (Fig. 4B), but did slightly improve R3616 replication in multi-step (MOI=0.1) replication assays in both cell lines (Fig. 4C).

Multi-step replication assays, using a low virus/cell ratio and longer timepoints (24 vs. 48 hpi), challenge the virus to undergo multiple rounds of replication and spread beyond the initially infected cells. The modest increases in viral titer observed in the multi-step assay (Fig 4C), but not the single-step assay, led us to hypothesize that uninfected cells in the multi-step assay benefitted to some degree from “pre-treatment” with ruxolitinib prior to becoming infected. To further test the effects of pre-treatment, the above experiments were repeated by exposing cells to ruxolitinib for 48 hrs followed by removal of the inhibitor prior to infection and addition of DMSO following infection. The results show that pre-treatment alone with ruxolitinib (Rux + DMSO) significantly improved the spread of C101 (Fig. 4D) as well as titers of R3616 in both single-step and multi-step assays in both cell lines (Fig. 4E–F) compared to DMSO pre-treatment (DMSO + DMSO). Interestingly, pre-treatment alone, whereby cells were washed of ruxolitinib prior to infection did not inhibit subsequent oHSV-induced STAT1 phosphorylation (Fig. 4G). Sequential pre-and co-treatment with ruxolitinib (Rux +Rux) further improved viral spread beyond pre-treatment alone (Fig. 4 D), however, it did not significantly improve viral replication in either the single-step or multi-step viral recovery assays (Fig. 4 E–F). Similar improvements were obtained with a M002 series oHSV (8) (Supplemental Fig. 4). To explain the unique effects of pre-treatment, we hypothesized that ruxolitinib inhibited low-level stimulation and activation of the JAK/STAT pathway in the STS26T-luc and ST8814-luc cell lines. To test this hypothesis, we stably transduced these cell lines with a nano-luciferase reporter under the control of a series of ISRE promoter elements and showed that ruxolitinib diminished the basal (uninfected) ISRE reporter activity in a concentration-dependent manner relative to DMSO (Fig 4H). An assessment of protein expression by western blot revealed that the expression of five representative ISGs (MDA5, RIG-I, MX1, IFIT3, and OAS1) decreased following 48 hr treatment with ruxolitinib as compared to DMSO (Fig. 4I). We conclude that basal STAT1/ISRE promoter activity leads to ISG expression which negatively impacts the productive infection of oHSVs.

Effect of ISG upregulation on oHSVs

To determine the extent to which basal ISGs expression occurs among other MPNST cell lines, we evaluated the relative levels of five ISGs (MDA5, RIG-I, MX1, IFIT3, and OAS1)

by immunoblot in all human MPNST cell lines. The results show that for the 5 probed ISGs, greater protein expression was detected in the cell lines ST8814-luc, T265-luc, 2XSB, STS26T-luc, and 90-8-luc whereas YST-1, NMS2-PC, and S462-luc had low or undetectable ISG expression (Fig 5A). The low ISG expression in S462-luc is notable since this cell line was the most permissive to oHSV infection producing the highest viral titers of MPNST cell lines tested. We hypothesized that higher basal ISG expression would increase oHSV resistance in S462-luc. To test this, S462-luc cells were exposed to different concentrations of IFN-β for 24 hrs and probed for ISGs by western blot. Fig 5B shows the associated increase in ISG expression with increasing concentrations of IFN-β, whereas IFN-β treated cells which were infected with C101 in a multi-step assay were less supportive of cell to cell spread in a manner dependent on the concentration of IFN-β. Because ISGs are only transiently expressed in S462-luc in response to IFN-β (data not shown) we stably co-expressed the ISGF3 component transcription factors (STAT1, STAT2, and IRF9), a strategy which has previously been reported to elevate basal ISG expression (11). Overexpression of ISGF3 in S462-luc similarly resulted in increased ISG expression (Fig 5C) and was associated with greater than 10 fold reduction of R3616 titers in both single-step and multi-step replication assays (Fig. 5D). We conclude that elevated ISG expression in MPNST cell lines diminishes oHSV productivity.

NFκB signaling and basal ISG expression

Recent reports have implicated the transcription factor NFκB, specifically the p65/RelA subunit, in promoting low level expression of IFNβ resulting in higher basal ISG expression (12). We hypothesized that MPNST cell lines with constitutively active NFκB increased ISG expression in oHSV resistant cell lines. To assess this, immunoblots were performed and showed relatively high p65 phosphorylation in the resistant cell lines STS26T-luc and ST8814-luc (Fig. 6A) suggesting elevated NFκB activity. To identify if basal ISRE transcriptional activity and ISG expression was related to NFκB transcriptional activity, we stably expressed nuclear factor of kappa light polypeptide gene enhancer in B-cells inhibitor, alpha (NFKBIA) (commonly known as inhibitor of κB; IκB), a native inhibitor of NFκB, with S32A/S36A mutations that prevent proteasomal degradation and act as an NFκB “super repressor.” The results show that IκB-super repressor (IκB-SR) expression decreases both NFκB and ISRE reporter activity (Fig. 6B). In contrast, control transduction had no effect upon NFκB or ISRE activity. IκB-SR expression also led to decreased expression of ISGs (Fig 6C). Together these results suggest that constitutive stimulation of the NFκB pathway can be related to the basal stimulation of ISRE elements and ISG expression.

Previous reports have shown that the small-molecule inhibitor TPCA-1, a dual inhibitor of IkB kinase (IKK) (a positive regulator of NFκB) and JAK1, can benefit the productivity of the oncolytic viruses vesicular stomatitis virus (VSV) and encephalomyocarditis virus (EMCV) (13, 14). We hypothesized that TPCA-1 could also benefit oHSV by downregulating expression of ISGs. Indeed, TPCA-1 inhibited the activity of both NFκB (Fig. 6D) and ISRE (Fig 6E) nano-luciferase reporters in a concentration dependent manner and reduced ISG expression in the treated cells (Fig. 6F). To test the effect of TPCA-1 on oHSV productivity, we used combinations of pre-treatment and co-treatment with TPCA-1 or DMSO, similar to the ruxolitinib studies described above. As with ruxolitinib, co-

treatment (DMSO + TPCA1) with TPCA-1 did not significantly improve $\Delta\gamma_1$34.5 infection and spread, however, pre-treatment (TPCA1 + DMSO) was sufficient to significantly improve the spread of both of the $\Delta\gamma_1$34.5 recombinants C101 and M201 in the ST8814-luc and STS26T-luc cell lines (Fig. 6 G–H). Interestingly, in contrast to the C101 and M201, the $\Delta\gamma_1$34.5 PKR evasion virus C154 benefited from either TPCA-1 co-treatment or from pre-treatment alone (Fig. 6I). Pre-treatment followed by co-treatment (TPCA1 + TPCA1) further improved spread in the majority of conditions tested.

DISCUSSION

The oHSVs engineered within our lab are derived from HSV-1 mutants with dual deletions of the $\gamma_1$34.5 neurovirulence gene rendering them safe to administer in the CNS (15). While normal cells restrict $\Delta\gamma_1$34.5 oHSV replication, a partial explanation for the oncolytic selectivity of $\Delta\gamma_1$34.5 HSVs for cancerous tissue is that malignant transformation of these cells results in an aberrant anti-viral response that complements viral loss of the $\gamma_1$34.5 gene. However, despite the wide variety of cancer types that are susceptible to oHSVs, resistance is commonly observed. In an *in vivo* setting, resistance can be attributed to inefficient delivery methods, low interstitial penetration, tumor heterogeneity, and activation of the innate and adaptive immune response. However, resistance is observed *in vitro.* This implies that the cancer cells themselves can independently restrict or resist oHSV infection and replication through intrinsic mechanisms.

Our previous work showed that the abundance of viral entry receptors was not responsible for restricted oHSV replication and growth in MPNST tumor cells (4). This suggests that an intracellular response contributes to intrinsic oHSV restriction. There are conflicting reports regarding the role of Ras signaling and its benefit to oHSV in the context of MPNSTs (16, 17). Our determination of the MEK/ERK status (Supplemental Fig. 5) shows that this pathway can be activated in both permissive and resistant MPNST cell lines similar to what was reported by Mahller *et al.* (16). Together with our observations regarding PKR, this suggests that Ras/MEK/ERK and PKR status are not sufficient to explain oHSV resistance in MPNST cells. Furthermore, an oHSV capable of evading the PKR response, C134, was also restricted in resistant MPNST cell lines despite inhibiting PKR activation. While PKR-mediated translational arrest is a critical obstacle, it appears not to be the sole impediment to $\Delta\gamma_1$34.5 oHSV replication in MPNST cells.

We demonstrated that viral productivity in MPNST tumor lines was inversely associated with an oHSV-induced STAT1 response; however, STAT1 inhibition using ruxolitinib during HSV infection did not improve oHSV replication and spread. Instead, ruxolitinib pre-treatment was necessary and sufficient to improve oHSV productivity. One potential explanation for the observable STAT1 response in oHSV resistant cells is that these cells have a greater basal upregulation of ISGs. A subset of ISGs are pattern recognition receptors (e.g. MDA5 and RIG-I) which lead to the expression of Type-I IFN and subsequent phosphorylation of STAT1 in response to infection. This capacity to respond to oHSV infection with STAT1 phosphorylation may therefore reflect (or act as a surrogate marker for) the co-expression of other ISGs which are directly antagonistic to oHSV replication and spread. Therefore suppressing the STAT1 response at the time of infection with ruxolitinib

co-treatment is insufficient to improve oHSV replication because basal ISG accumulation is sufficient to impart this viral resistance. The downregulation of basal ISRE activity and ISG expression following ruxolitinib pre-treatment supports the hypothesis that reduced accumulation of antiviral effectors is sufficient to improve oHSV infection and spread. The presence of faint p-Y701 STAT1 staining in some of the uninfected resistant MPNST cell lines (e.g. STS26T-luc and A382 in Fig 2A) supports the possibility that basal STAT1 activity contributes to the expression of ISGs in these cell lines. Finally, consistent with our observation that viral productivity of both $\Delta\gamma_1$34.5 (9, 18) and C134 ($\Delta\gamma_1$34.5 IRS1) are associated with the capacity for a STAT1 response, these viruses have been previously been reported to be sensitive to Type-I IFN pretreatment (9, 18) while wild-type HSV-1 remains insensitive to those effects (9, 18).

While basal expression of ISGs has been previously documented in a number of tumor-derived cell lines (19–23), this has not been shown for MPNSTs. However in the context of oHSV infection, Mahller *et al.* showed through gene expression analysis that the “JAK/STAT pathway” and “Tyrosine Phosphorylation of STAT protein” were significantly upregulated in response to G207 (a lacZ expressing variant of R3616) in a panel of MPNST cell lines (24). Interestingly, knockdown of suppressor of cytokine signaling 1 (SOCS1), a negative regulator of STAT1, decreased the viral titers of the G207 by more than 10 fold in the highly permissive cell line S462.

Activation of the JAK/STAT pathway and ISG expression limits other oncolytic viruses including vesicular stomatitis virus (13, 19,22, 23, 25), measles virus (20), Newcastle Disease virus (21), respiratory syncytial virus (26), Semliki Forest virus (27), and adenovirus (28, 29). In several of these studies inhibitors of JAK/STAT1 signaling enhanced viral productivity (19, 22,23, 25, 27). With respect to HSV, a head and neck squamous cell carcinoma, which became radio-resistant through the upregulation of STAT1 and other ISGs, suppressed the replication of oHSV R3616 by 40 fold compared to the original tumor (30). Haseley *et al.* found that overexpression of the extracellular matrix protein cysteine rich 61 (CYR61) induced upregulation of type-1 IFNs and ISGs which suppressed oHSV productivity in glioma cells (31). Although $\Delta\gamma_1$34.5 HSVs are known to be sensitive to exogenous IFN (9, 18), presumably through the upregulation of ISGs by STAT1, these appear to be the only reports in the literature between a cancer-associated STAT1/ISG signature and resistance to oHSV.

The STAT1/ISG expression signature has been detected in a number of patient tumor specimens including glioblastoma (32, 33), squamous cell carcinoma (34), melanoma (35), leukemia (36), breast (36–38), ovarian (36), and pancreatic (28) cancers suggesting that cancer-associated STAT1/ISG expression is not an *in vitro* artifact. In these reports it is not possible to determine whether the STAT1 signature is a phenotype driven by the intrinsic nature of the tumor cells (autocrine activation) or whether expression of this signature occurs in response to inflammatory stimuli from the surrounding microenvironment (paracrine activation). Regardless of the mechanism, STAT1 and ISG expression signatures have been implicated in the resistance of cancer to radiation (30, 39, 40) and chemotherapy (39, 41, 42). ISG expression in MPNSTs may offer a possible explanation for the lack of efficacy by these treatment modalities in patients with MPNSTs (2, 3).

It has been shown that innate immune effectors including microglia, macrophages, and natural killer cells actively restrict replication of oncolytic HSV *in vivo* (43, 44). However, oncolytic viruses may be beneficial as an immunotherapy by provoking an immune response, specifically involving natural killer cells and cytotoxic T cells, leading to recognition and clearance of the tumor, despite the detriment to viral replication and oncolysis (45, 46). Indeed, paradoxical responses to oHSV have been reported whereby tumor cells which were characterized as oHSV resistant *in vitro* were more susceptible to the anti-tumor effect of oHSV *in vivo* (46). While we have demonstrated associated STAT1 activation to be detrimental to oHSV productivity *in vitro*, it will be necessary to identify how tumor cells that are STAT1 responsive interact with the peripheral immune elements in this context since the efficacy of certain immunotherapies and the recruitment of CTLs is dependent upon the Type-I IFN response (47). Additionally, the use of powerful immunosuppressants such as JAK inhibitors may counteract the effects of immunotherapy or diminish the safety profiles which have been previously established for oHSV.

Finally, the driver for basal ISG expression in tumor cells remains incompletely understood. Virally induced NFκB activation is known to promote IFNβ transcription (48), but the extent to which the constitutive NFκB activation, which is commonly overserved in certain cancers, affects IFNβ expression is unclear. There is some evidence that upstream signaling components of the NFκB pathway, independent of NFκB-driven gene expression, may be involved in STAT1 cross-talk (49, 50). Further work is needed to determine the prevalence of NFκB-related ISG expression and the complete mechanism in MPNSTs.

In conclusion, our current research has identified a previously unexplored component of MPNST resistance to $\Delta\gamma_1$34.5 oHSVs. We believe the novel finding of basal ISG expression in MPNST cells may have further implications for MPNST biology and their treatment with conventional anti-tumor therapies.

Supplementary Material

Refer to Web version on PubMed Central for supplementary material.

Acknowledgments

Special thanks to the UAB Comprehensive Flow Cytometry Core, UAB Heflin Genetics Center for Genomic Science, and Dr. Bernard Roizman (University of Chicago, Chicago, IL) for providing R3616.

FUNDING: Funding for this research was provided through DOD-W81XWH-10-NFRP-IIRA-NF1001157, P20 CA151129-03, P01 CA71933-15 and P50 CA97247-05.

REFERENCES

1. Kolberg M, Høland M, Ågesen TH, Brekke HR, Liestøl K, Hall KS, et al. Survival meta-analyses for >1800 malignant peripheral nerve sheath tumor patients with and without neurofibromatosis type 1. Neuro-oncology. 2013; 15:135–147. [PubMed: 23161774]
2. Wong WW, Hirose T, Scheithauer BW, Schild SE, Gunderson LL. Malignant peripheral nerve sheath tumor: analysis of treatment outcome. Int J Radiat Oncol Biol Phys. 1998; 42:351–360. [PubMed: 9788415]

3. Zehou O, Fabre E, Zelek L, Sbidian E, Ortonne N, Banu E, et al. Chemotherapy for the treatment of malignant peripheral nerve sheath tumors in neurofibromatosis 1: a 10-year institutional review. Orphanet J Rare Dis. 2013; 8:127. [PubMed: 23972085]
4. Jackson JD, McMorris AM, Roth JC, Coleman JM, Whitley RJ, Gillespie GY, et al. Assessment of oncolytic HSV efficacy following increased entry-receptor expression in malignant peripheral nerve sheath tumor cell lines. Gene Ther. 2014; 21:984–990. [PubMed: 25119379]
5. Farassati F, Yang A-D, Lee PW. Oncogenes in Ras signalling pathway dictate host-cell permissiveness to herpes simplex virus 1. Nat Cell Biol. 2001; 3:745–750. [PubMed: 11483960]
6. Cassady KA. Human cytomegalovirus TRS1 and IRS1 gene products block the double-stranded-RNA-activated host protein shutoff response induced by herpes simplex virus type 1 infection. J Virol. 2005; 79:8707–8715. [PubMed: 15994764]
7. Kazmi SJ, Byer SJ, Eckert JM, Turk AN, Huijbregts RP, Brossier NM, et al. Transgenic mice overexpressing neuregulin-1 model neurofibroma-malignant peripheral nerve sheath tumor progression and implicate specific chromosomal copy number variations in tumorigenesis. Am J Pathol. 2013; 182:646–667. [PubMed: 23321323]
8. Parker JN, Gillespie GY, Love CE, Randall S, Whitley RJ, Markert JM. Engineered herpes simplex virus expressing IL-12 in the treatment of experimental murine brain tumors. Proc Natl Acad Sci USA. 2000; 97:2208–2213. [PubMed: 10681459]
9. Cheng G, Brett M-E, He B. Val 193 and Phe 195 of the γ 1 34.5 protein of herpes simplex virus 1 are required for viral resistance to interferon-α/β. Virology. 2001; 290:115–120. [PubMed: 11882996]
10. Shah A, Parker J, Gillespie G, Lakeman F, Meleth S, Markert J, et al. Enhanced antiglioma activity of chimeric HCMV/HSV-1 oncolytic viruses. Gene Ther. 2007; 14:1045–1054. [PubMed: 17429445]
11. Cheon H, Holvey-Bates EG, Schoggins JW, Forster S, Hertzog P, Imanaka N, et al. IFNbeta-dependent increases in STAT1, STAT2, and IRF9 mediate resistance to viruses and DNA damage. EMBO J. 2013; 32:2751–2763. [PubMed: 24065129]
12. Basagoudanavar SH, Thapa RJ, Nogusa S, Wang J, Beg AA, Balachandran S. Distinct roles for the NF-κB RelA subunit during antiviral innate immune responses. J Virol. 2011; 85:2599–2610. [PubMed: 21209118]
13. Cataldi M, Shah NR, Felt SA, Grdzelishvili VZ. Breaking resistance of pancreatic cancer cells to an attenuated vesicular stomatitis virus through a novel activity of IKK inhibitor TPCA-1. Virology. 2015; 485:340–354. [PubMed: 26331681]
14. Du Z, Whitt MA, Baumann J, Garner JM, Morton CL, Davidoff AM, et al. Inhibition of type I interferon-mediated antiviral action in human glioma cells by the IKK inhibitors BMS-345541 and TPCA-1. J Interferon Cytokine Res. 2012; 32:368–377. [PubMed: 22509977]
15. Chou J, Kern ER, Whitley RJ, Roizman B. Mapping of herpes simplex virus-1 neurovirulence to gamma 134.5, a gene nonessential for growth in culture. Science. 1990; 250:1262–1266. [PubMed: 2173860]
16. Mahller YY, Rangwala F, Ratner N, Cripe TP. Malignant peripheral nerve sheath tumors with high and low Ras-GTP are permissive for oncolytic herpes simplex virus mutants. Pediatr Blood Cancer. 2006; 46:745–754. [PubMed: 16124003]
17. Farassati F, Pan W, Yamoutpour F, Henke S, Piedra M, Frahm S, et al. Ras signaling influences permissiveness of malignant peripheral nerve sheath tumor cells to oncolytic herpes. Am J Pathol. 2008; 173:1861–1872. [PubMed: 18988803]
18. Cassady KA, Saunders U, Shimamura M. Δγ134. 5 Herpes Simplex Viruses Encoding Human Cytomegalovirus IRS1 or TRS1 Induce Interferon Regulatory Factor 3 Phosphorylation and an Interferon-Stimulated Gene Response. J Virol. 2012; 86:610–614. [PubMed: 22072777]
19. Paglino JC, van den Pol AN. Vesicular stomatitis virus has extensive oncolytic activity against human sarcomas: rare resistance is overcome by blocking interferon pathways. J Virol. 2011; 85:9346–9358. [PubMed: 21734048]
20. Berchtold S, Lampe J, Weiland T, Smirnow I, Schleicher S, Handgretinger R, et al. Innate immune defense defines susceptibility of sarcoma cells to measles vaccine virus-based oncolysis. J Virol. 2013; 87:3484–3501. [PubMed: 23302892]

21. Wilden H, Fournier P, Zawatzky R, Schirrmacher V. Expression of RIG-I, IRF3, IFN-β and IRF7 determines resistance or susceptibility of cells to infection by Newcastle Disease Virus. Int J Oncol. 2009; 34:971–982. [PubMed: 19287954]
22. Escobar-Zarate D, Liu Y, Suksanpaisan L, Russell S, Peng K. Overcoming cancer cell resistance to VSV oncolysis with JAK1/2 inhibitors. Cancer Gene Ther. 2013; 20:582–589. [PubMed: 24030211]
23. Moerdyk-Schauwecker M, Shah NR, Murphy AM, Hastie E, Mukherjee P, Grdzelishvili VZ. Resistance of pancreatic cancer cells to oncolytic vesicular stomatitis virus: role of type I interferon signaling. Virology. 2013; 436:221–234. [PubMed: 23246628]
24. Mahller Y, Sakthivel B, Baird W, Aronow B, Hsu Y, Cripe T, et al. Molecular analysis of human cancer cells infected by an oncolytic HSV-1 reveals multiple upregulated cellular genes and a role for SOCS1 in virus replication. Cancer Gene Ther. 2008; 15:733–741. [PubMed: 18551144]
25. Liu Y-P, Suksanpaisan L, Steele MB, Russell SJ, Peng K-W. Induction of antiviral genes by the tumor microenvironment confers resistance to virotherapy. Sci Rep. 2013; 3
26. Echchgadda I, Chang T-H, Sabbah A, Bakri I, Ikeno Y, Hubbard GB, et al. Oncolytic targeting of androgen-sensitive prostate tumor by the respiratory syncytial virus (RSV): consequences of deficient interferon-dependent antiviral defense. BMC cancer. 2011; 11:43. [PubMed: 21276246]
27. Ruotsalainen J, Kaikkonen M, Niittykoski M, Martikainen M, Lemay C, Cox J, et al. Clonal variation in interferon response determines the outcome of oncolytic virotherapy in mouse CT26 colon carcinoma model. Gene Ther. 2014
28. Monsurrò V, Beghelli S, Wang R, Barbi S, Coin S, Di Pasquale G, et al. Anti-viral state segregates two molecular phenotypes of pancreatic adenocarcinoma: potential relevance for adenoviral gene therapy. J Transl Med. 2010; 8:10. [PubMed: 20113473]
29. Liikanen I, Monsurrò V, Ahtiainen L, Raki M, Hakkarainen T, Diaconu I, et al. Induction of interferon pathways mediates in vivo resistance to oncolytic adenovirus. Mol Ther. 2011; 19:1858–1866. [PubMed: 21792178]
30. Khodarev NN, Beckett M, Labay E, Darga T, Roizman B, Weichselbaum RR. STAT1 is overexpressed in tumors selected for radioresistance and confers protection from radiation in transduced sensitive cells. Proc Natl Acad Sci U S A. 2004; 101:1714–1719. [PubMed: 14755057]
31. Haseley A, Boone S, Wojton J, Yu L, Yoo JY, Yu J, et al. Extracellular Matrix Protein CCN1 Limits Oncolytic Efficacy in Glioma. Cancer Res. 2012; 72:1353–1362. [PubMed: 22282654]
32. Duarte CW, Willey CD, Zhi D, Cui X, Harris JJ, Vaughan LK, et al. Expression signature of IFN/STAT1 signaling genes predicts poor survival outcome in glioblastoma multiforme in a subtype-specific manner. PLoS One. 2012; 7:e29653. [PubMed: 22242177]
33. Cosset É, Petty TJ, Dutoit V, Cordey S, Padioleau I, Otten-Hernandez P, et al. Comprehensive metagenomic analysis of glioblastoma reveals absence of known virus despite antiviral-like type I interferon gene response. Int J Cancer. 2014; 135:1381–1389. [PubMed: 24347514]
34. Laimer K, Spizzo G, Obrist P, Gastl G, Brunhuber T, Schäfer G, et al. STAT1 activation in squamous cell cancer of the oral cavity. Cancer. 2007; 110:326–333. [PubMed: 17559122]
35. Schultz J, Koczan D, Schmitz U, Ibrahim SM, Pilch D, Landsberg J, et al. Tumor-promoting role of signal transducer and activator of transcription (Stat) 1 in late-stage melanoma growth. Clin Exp Metastasis. 2010; 27:133–140. [PubMed: 20180146]
36. Einav U, Tabach Y, Getz G, Yitzhaky A, Ozbek U, Amariglio N, et al. Gene expression analysis reveals a strong signature of an interferon-induced pathway in childhood lymphoblastic leukemia as well as in breast and ovarian cancer. Oncogene. 2005; 24:6367–6375. [PubMed: 16007187]
37. Perou CM, Sørlie T, Eisen MB, van de Rijn M, Jeffrey SS, Rees CA, et al. Molecular portraits of human breast tumours. Nature. 2000; 406:747–752. [PubMed: 10963602]
38. Perou CM, Jeffrey SS, Van De Rijn M, Rees CA, Eisen MB, Ross DT, et al. Distinctive gene expression patterns in human mammary epithelial cells and breast cancers. Proc Natl Acad Sci USA. 1999; 96:9212–9217. [PubMed: 10430922]
39. Fryknäs M, Dhar S, Öberg F, Rickardson L, Rydåker M, Göransson H, et al. STAT1 signaling is associated with acquired crossresistance to doxorubicin and radiation in myeloma cell lines. Int J Cancer. 2007; 120:189–195. [PubMed: 17072862]

40. Tsai M-H, Cook JA, Chandramouli GV, DeGraff W, Yan H, Zhao S, et al. Gene expression profiling of breast, prostate, and glioma cells following single versus fractionated doses of radiation. Cancer Res. 2007; 67:3845–3852. [PubMed: 17440099]

41. Patterson S, Wei S, Chen X, Sallman D, Gilvary D, Zhong B, et al. Novel role of Stat1 in the development of docetaxel resistance in prostate tumor cells. Oncogene. 2006; 25:6113–6122. [PubMed: 16652143]

42. Luszczek W, Cheriyath V, Mekhail TM, Borden EC. Combinations of DNA methyltransferase and histone deacetylase inhibitors induce DNA damage in small cell lung cancer cells: correlation of resistance with IFN-stimulated gene expression. Mol Cancer Ther. 2010; 9:2309–2321. [PubMed: 20682643]

43. Kurozumi K, Hardcastle J, Thakur R, Yang M, Christoforidis G, Fulci G, et al. Effect of tumor microenvironment modulation on the efficacy of oncolytic virus therapy. J Natl Cancer Inst. 2007; 99:1768–1781. [PubMed: 18042934]

44. Ikeda K, Ichikawa T, Wakimoto H, Silver JS, Deisboeck TS, Finkelstein D, et al. Oncolytic virus therapy of multiple tumors in the brain requires suppression of innate and elicited antiviral responses. Nat Med. 1999; 5:881–887. [PubMed: 10426310]

45. Workenhe ST, Simmons G, Pol JG, Lichty BD, Halford WP, Mossman KL. Immunogenic HSV-mediated oncolysis shapes the antitumor immune response and contributes to therapeutic efficacy. Mol Ther. 2014; 22:123–131. [PubMed: 24343053]

46. Leddon JL, Chen C-Y, Currier MA, Wang P-Y, Jung FA, Denton NL, et al. Oncolytic HSV virotherapy in murine sarcomas differentially triggers an antitumor T-cell response in the absence of virus permissivity. Mol Ther Oncolytics. 2015; 1

47. Corrales L, Gajewski TF. Molecular Pathways: Targeting the Stimulator of Interferon Genes (STING) in the Immunotherapy of Cancer. Clin Cancer Res. 2015 clincanres. 1362.2015.

48. Wang J, Basagoudanavar SH, Wang X, Hopewell E, Albrecht R, García-Sastre A, et al. NF-κB RelA subunit is crucial for early IFN-β expression and resistance to RNA virus replication. J Immunol. 2010; 185:1720–1729. [PubMed: 20610653]

49. Ng S-L, Chua MA, McWhirter SM, García-Sastre A, Maniatis T. Multiple functions of the IKK-related kinase IKKε in interferon-mediated antiviral immunity. Science. 2007; 315:1274–1278. [PubMed: 17332413]

50. Nguyen H, Chatterjee-Kishore M, Jiang Z, Qing Y, Ramana CV, Bayes J, et al. IRAK-dependent phosphorylation of Stat1 on serine 727 in response to interleukin-1 and effects on gene expression. J Interferon Cytokine Res. 2003; 23:183–192. [PubMed: 12856330]

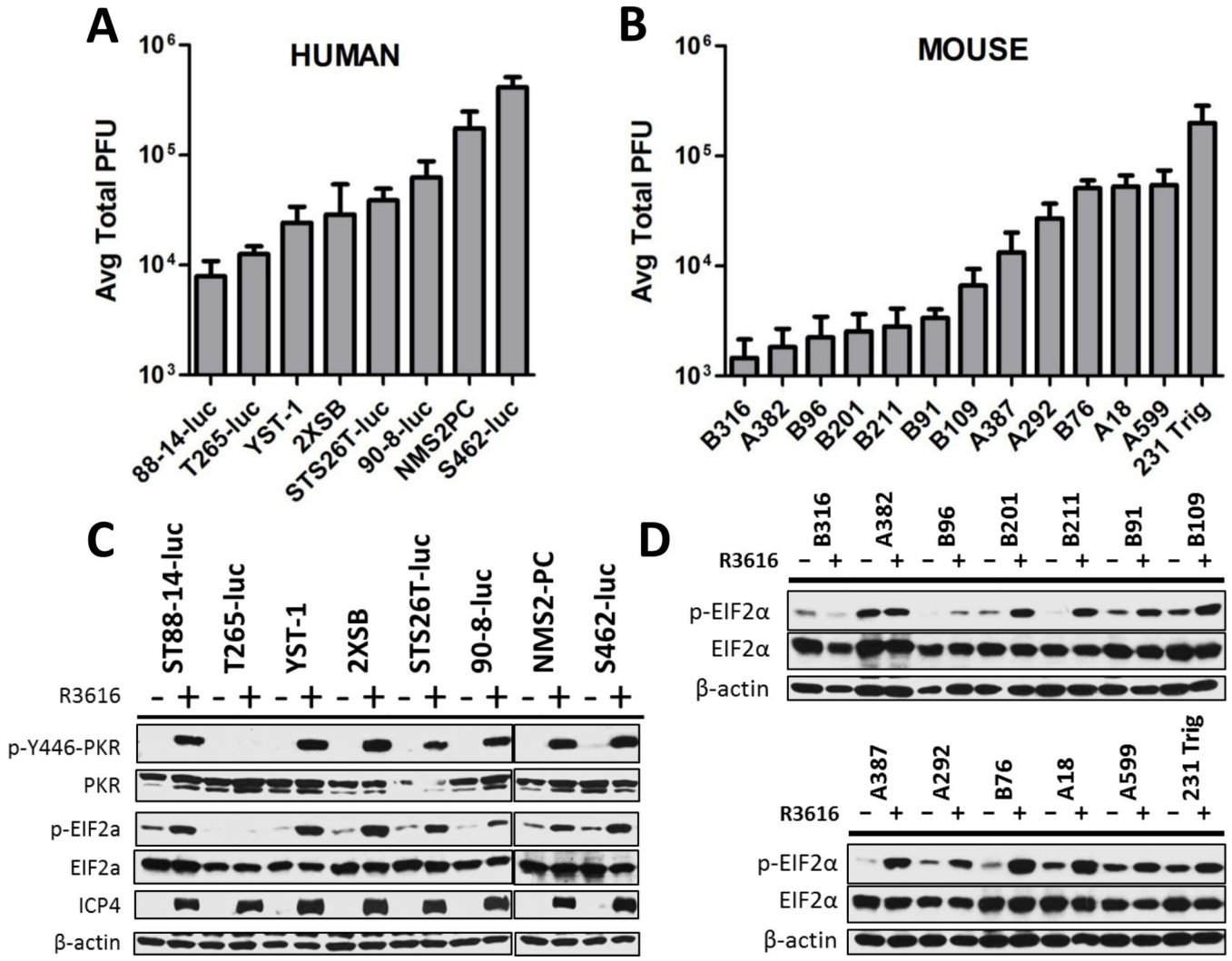

Figure 1. oHSV productivity and activation of the PKR response

Human (A) and mouse (B) derived MPNST cell lines were infected with R3616 (MOI=1, 24 hpi) and viral recovery measured using standard titration methods. Data were collected in triplicate and the titers are reported as the average total plaque forming units (PFU) with standard deviation. PKR and eIF2α in human cell lines (C) or eIF2α alone in mouse cell lines (D) was assessed by western blot for phosphorylation in response to mock or R3616 (MOI=1, 12 hpi) infection.

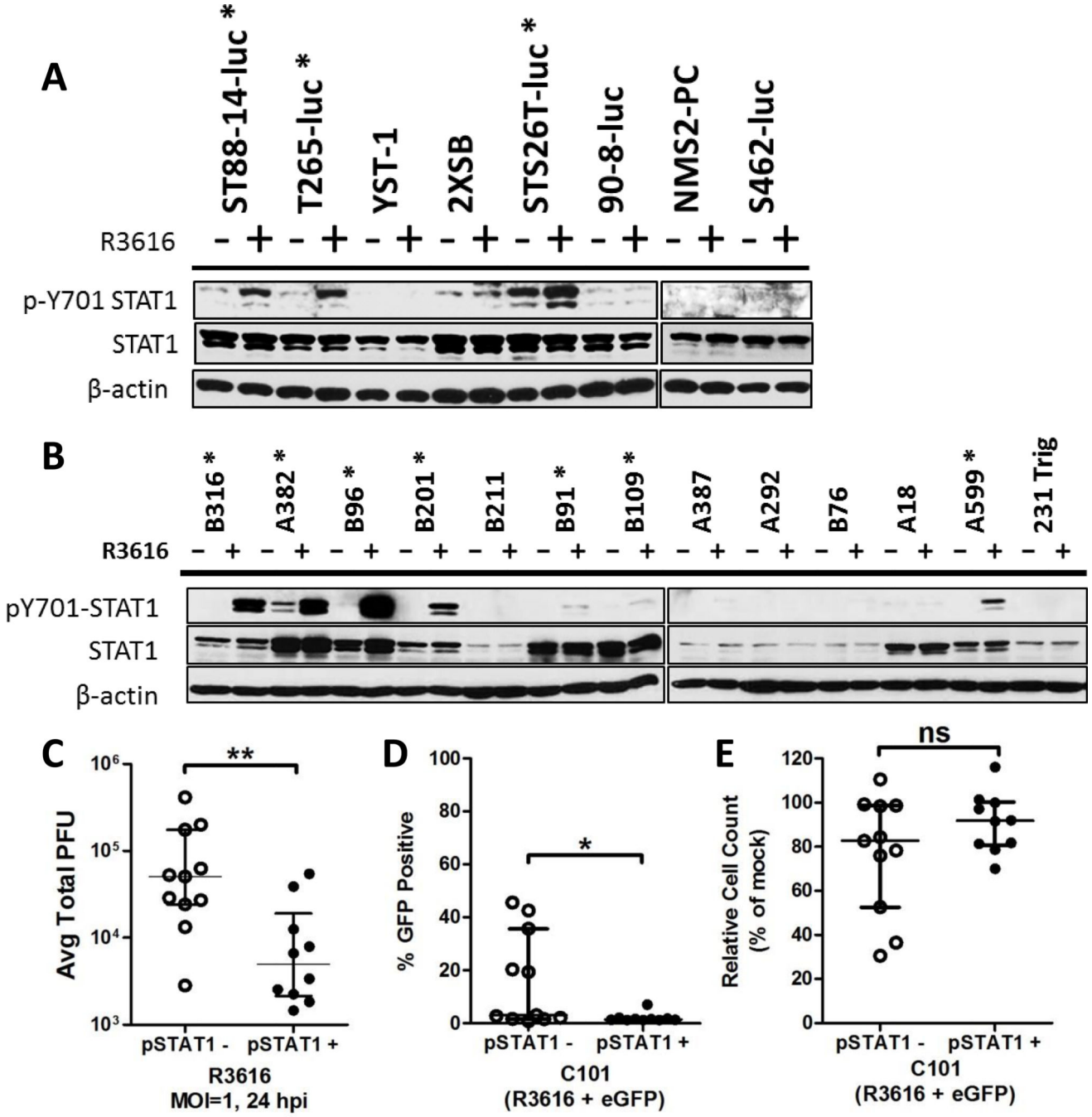

Figure 2. STAT1 response to oHSV infection and association with viral productivity

STAT1 phosphorylation in response to R3616 infection (MOI=1, 6hpi) was assessed by western blot in human (A) and mouse (B) cell lines. Cell lines considered STAT1 responsive are marked with an asterisk. The mean viral titers (from Fig. 1 A–B) from each cell line were sorted into STAT1 unresponsive and responsive groups and tested for statistical significance using the Mann-Whitney U test with the median and interquartile range plotted (C). Cell lines were assessed in a multistep infection assay (MOI=0.1, 48 hpi) with C101 for the percentage of cells positive for GFP (D) and the infected cell count as a percentage of the

mock infected cell count (E). Data were collected in triplicate and the mean reported. Cell lines were sorted based on their STAT1 response and tested for statistical significance using the Mann-Whitney U test with the medians and interquartile range plotted.

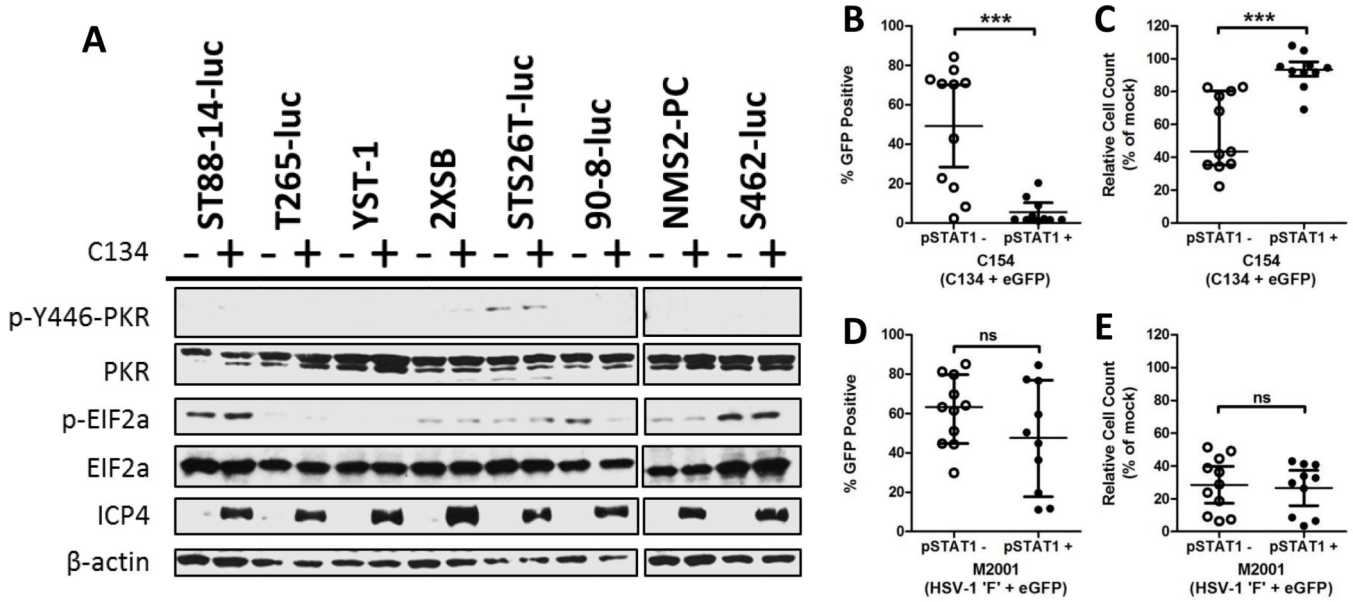

Figure 3. PKR activation with C134 and association of productivity with STAT1 response

PKR and eIF2α in human cell lines (A) was assessed by western blot for phosphorylation in response to mock or C134 (MOI=1, 12 hpi) infection. Cell lines were assessed in a multistep infection assay (MOI=0.1, 48 hpi) with C134 and M2001 for the percentage of cells positive for GFP (B and D) and the infected cell count as a percentage of the mock infected cell count (C and E). Data were collected in triplicate and the mean reported. Cell lines were sorted based on their STAT1 response and tested for statistical significance using the Mann-Whitney U test with the medians and interquartile range plotted.

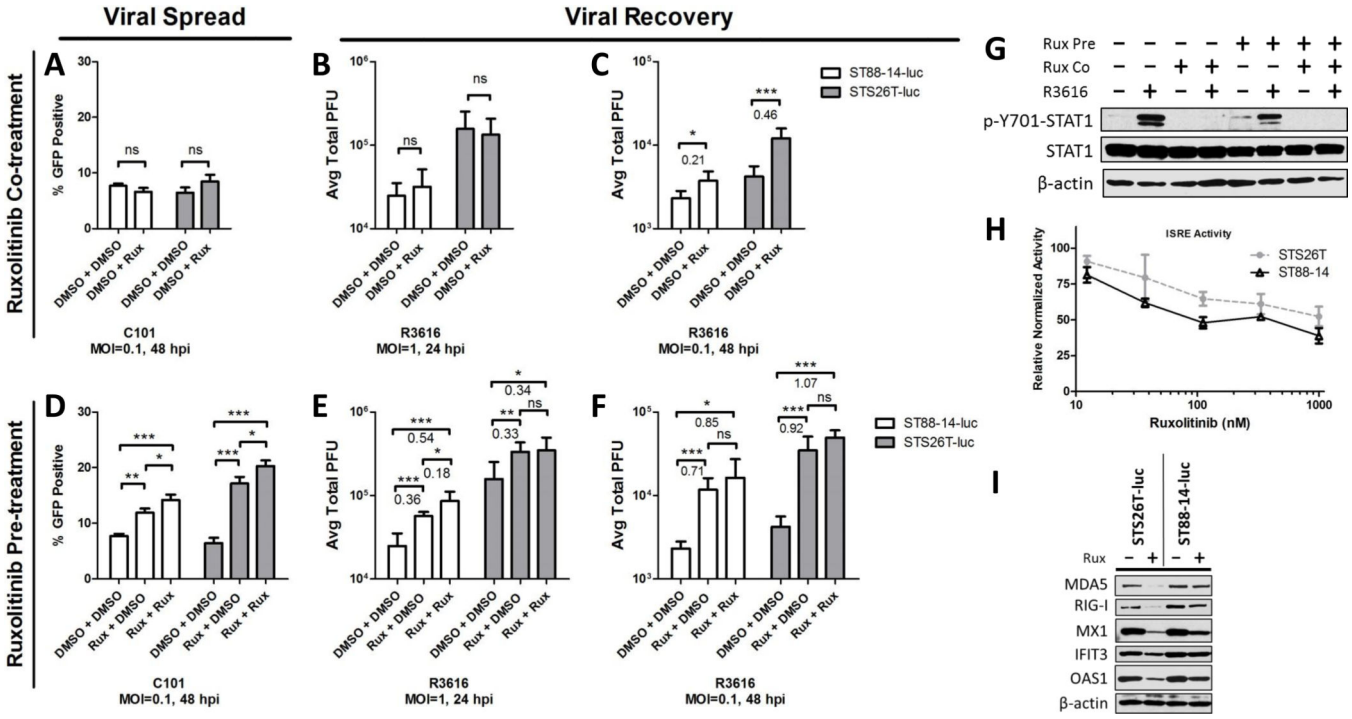

Figure 4. Effect of JAK inhibitor ruxolitinib on viral productivity, basal ISRE activity, and ISG expression

Cell lines were pretreated with either DMSO or 250 nM ruxolitinib (Rux) for 48 hrs prior to infection. One hour after oHSV infection, each group was further co-treated with DMSO or ruxolitinib (250 nM). GFP expressing virus C101 was used to assess effects on oHSV spread by multistep infection (MOI=0.1, 48 hpi) (A–B, E–F). Multistep (MOI=0.1, 48 hpi) (C and G) and single-step (MOI=1, 25 hpi) (D and H) infection with R3616 was used to assess viral recovery. Data for spread and recovery assays were collected in triplicate and the standard deviation reported. For viral recovery, the log-fold change is reported under the significance indicator. Phosphorylation of STAT1 was observed by western blot in ST88-14-luc treated with combinations of DMSO and ruxolitinib (I). ISRE activity was measured by dual luciferase assays after 24 hr treatment with various concentrations of ruxolitinib (J). ISRE nanoluciferase activity was normalized to that of firefly luciferase and final values reported as the percentage of DMSO treated cells. Expression of ISGs MDA5, RIG-I, MX1, IFIT3, and OAS1 in cell lines treated with DMSO or ruxolitinib (250 nM) for 48 hrs was observed by western blot (K).

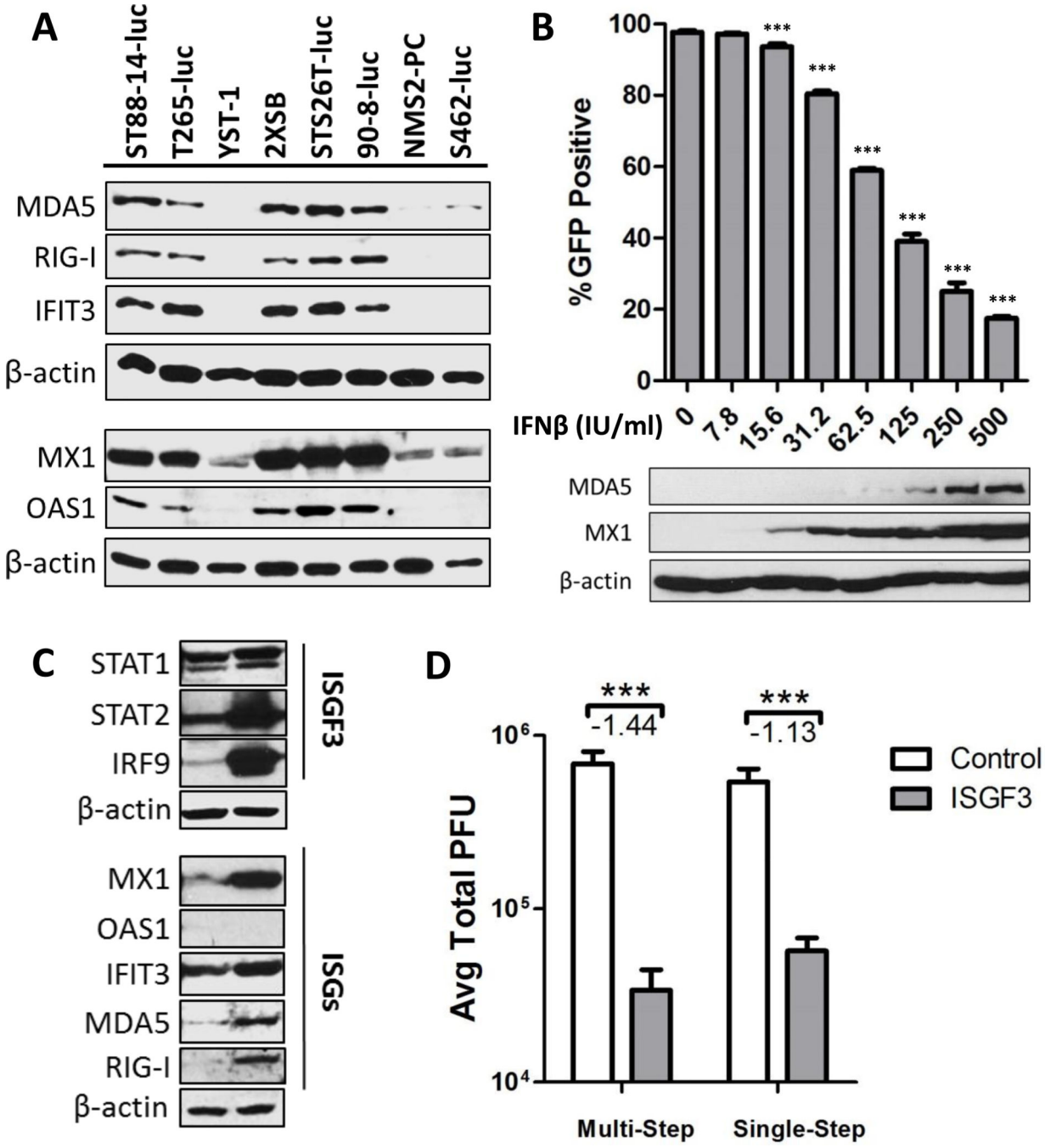

Figure 5. Basal expression of ISGs in MPNST cell lines and effect of increased ISG expression on viral productivity

Basal expression of ISGs in all human MPSNT cell lines was assessed by western blot (A). S462-luc cells were treated with IFN-β for 24 hr and subsequently probed by immunoblot for ISGs (B) or infected with C101 at MOI=0.2. Infected cells were then assessed by FACS for the percentage of cells positive for viral eGFP at 48 hpi (B). S462-luc was stably transduced with a control lentivirus (DsRed2) or lentiviruses encoding the transcription factors STAT1-FLAG, STAT2 and IRF9 which compose the ISGF3 complex were assessed for ISG expression by western blot (C). Multi-step (MOI=0.1, 48 hpi) and single-step

(MOI=1, 24 hpi) (D) viral recovery assays with R3616 were conducted in control and ISGF3 transduced cell lines. In each described assay, data were collected in triplicate and the standard deviation reported. The log-fold change is reported under the significance indicator.

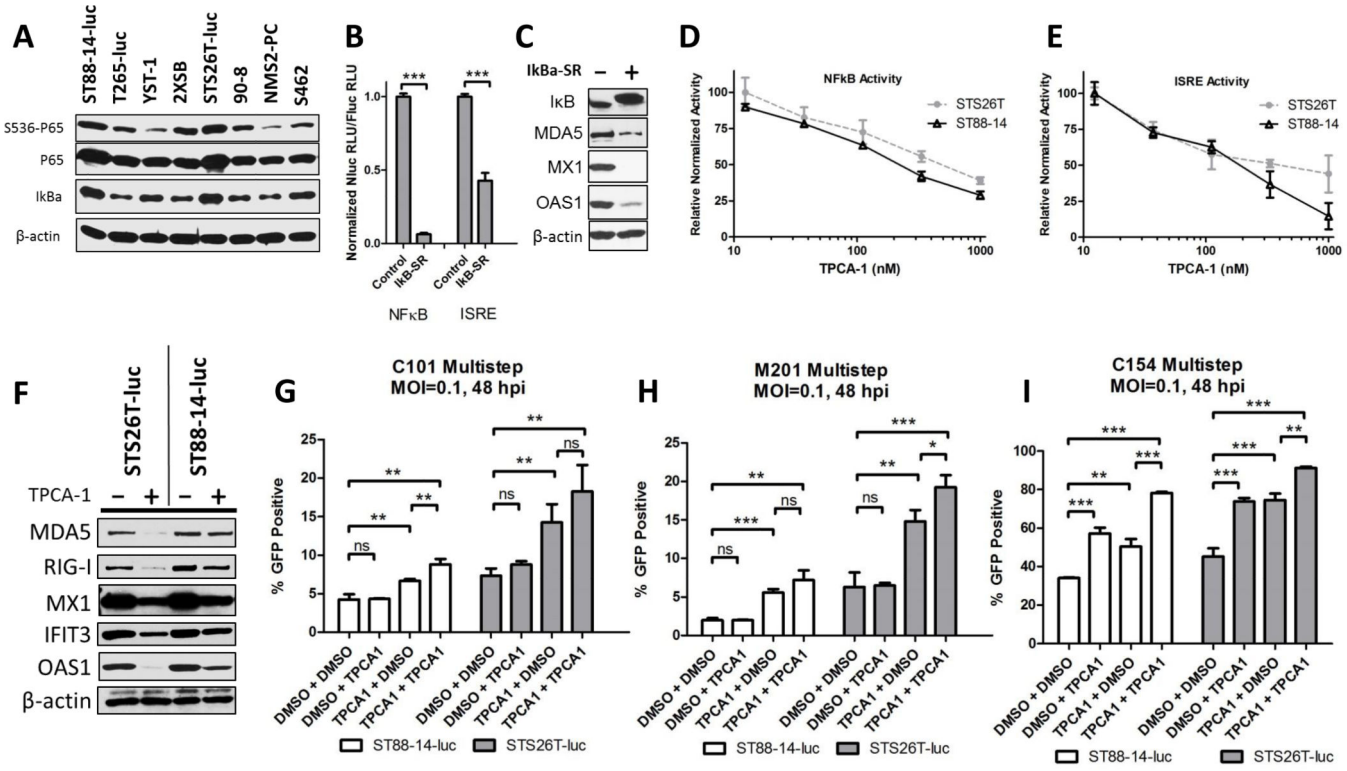

Figure 6. Relationship of NFκB to basal ISG expression

Phosphorylation of P65/RelA was assessed in human cell lines by western blot (A). The cell line ST88-14-luc expressing either NFκB or ISRE luciferase reporters were stably transduced with the inhibitor of kB super repressor (IkB-SR) and nano-luciferase (Nluc) activity measured (B). Firefly luciferase (Fluc) normalized data were collected in quadruplicate and standard deviation reported. IkB-SR transduced ST88-14-luc was probed for IkB and ISG expression by western blot (C). NFκB (D) and ISRE (E) luciferase activity was measured in response to the small molecule inhibitor TPCA-1. Firefly luciferase normalized data were collected in triplicate and the percentage of activity relative to DMSO treatment was reported with standard deviation. Expression of ISGs was probed in TPCA-1 treated cell lines (250 nM, 96 hr) by western blot (F). Cell lines were pretreated with either DMSO or 250 nM TPCA-1 (Rux) for 96 hrs prior to infection. One hour after oHSV infection, each group was further co-treated with DMSO or TPCA-1 (250 nM). GFP expressing viruses C101 (G), M201 (H), and C134 (I) were used to assess effects on oHSV spread by multistep infection (MOI=0.1, 48 hpi). Data were collected in triplicate and the standard deviation reported.